Resonant phonon modes in ultra-thin superlattice structures

1989 J. Phys.: Condens. Matter 1 2445

(http://iopscience.iop.org/0953-8984/1/13/016)

J. Phys.: Condens. Matter 1 (1989) 2445–2450. Printed in the UK

LETTER TO THE EDITOR

Resonant phonon modes in ultra-thin superlattice structures

M W C Dharma-wardana, D J Lockwood, G C Aers and J-M Baribeau
Division of Physics, National Research Council, Ottawa, Ontario K1A 0R6, Canada

Received 31 May 1988, in final form 24 January 1989

Abstract. Raman scattering from acoustic phonons in Ge_mSi_n ultra-thin superlattices grown on (001) Si substrates is reported. We identify unexpectedly intense broad peaks in the low-frequency spectrum with resonant phonon modes arising from substrate–superlattice interactions. A linear chain model is used to simulate the spectrum and it reveals the importance of substrate–superlattice interactions and surface boundary conditions for intensity calculations in these superlattices.

Impressive developments in molecular beam epitaxial (MBE) growth techniques have led to the creation of a variety of solid state structures not obtainable via conventional methods. Very recently, ultra-thin, strained-layer superlattices with only a few atomic layers per period along the growth direction have been fabricated (Bevk *et al* 1986). Thus ordered systems of the form A_mB_n, with m monolayers of A and n monolayers of B, where for example, A ≡ Ge, B ≡ Si, $n = 2$, $m = 2$, have been made, although such structures are not conventionally stable (Flynn 1986). The impetus for the preparation and study of such novel materials arises from the possibility of their having entirely new properties as compared with those of the parent materials.

Here we report a Raman scattering study of several ultra-thin Ge_mSi_n superlattices grown by MBE on (001) Si substrates. The thin films were deposited in a VG V 80 system using procedures described previously (Houghton *et al* 1987). Si and Ge fluxes were produced by electron beam evaporation. The deposition rates were carefully calibrated using crystal monitors and were continuously controlled during the growth by Inficon Leybold–Heraus Sentinel sensors. All the layers were grown at 500 °C with a typical growth rate of about 0.2 Å s^{-1}. For the present study three multilayer structures consisting of 15 periods of Ge_2Si_2, 10 periods of Ge_2Si_2, and 8 periods of Ge_4Si_4 were prepared. With the last superlattice, a portion of the wafer surface was capped with a Si layer of thickness approximately 150 Å. All these samples have thicknesses of less than 100 Å and do not exceed the critical thickness for plastic relaxation (Bevk *et al* 1986). We also studied a comparable sample (thickness 80 Å) of a partially relaxed, random alloy layer of nominal composition $Ge_{0.5}Si_{0.5}$. The 'free surfaces' of these superlattices are nominally silicon layers, but in practice at least the last two layers would be affected by oxidation and accretion of impurities.

The Raman spectra were measured in a 90° scattering geometry with the sample (001) surface inclined at an angle of 12.3° to the incident light (Lockwood *et al* 1987). The large refractive index of these materials makes this effectively a backscattering

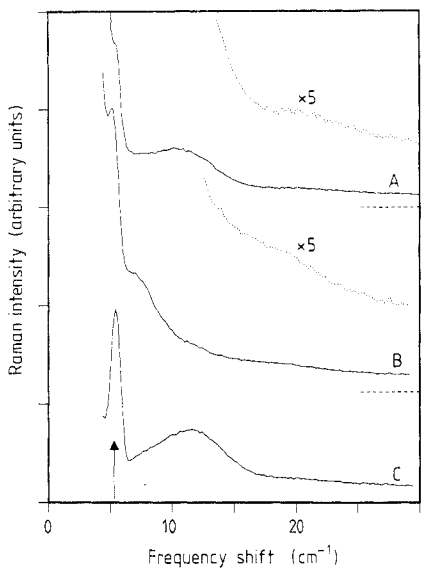

Figure 1. The experimental Raman spectra of samples A (15 periods of Ge_2Si_2), B (8 periods of Ge_4Si_4) and C (10 periods of Ge_2Si_2). The Brillouin frequency $\omega_{Br} = 5.3\ cm^{-1}$ is marked with an arrow.

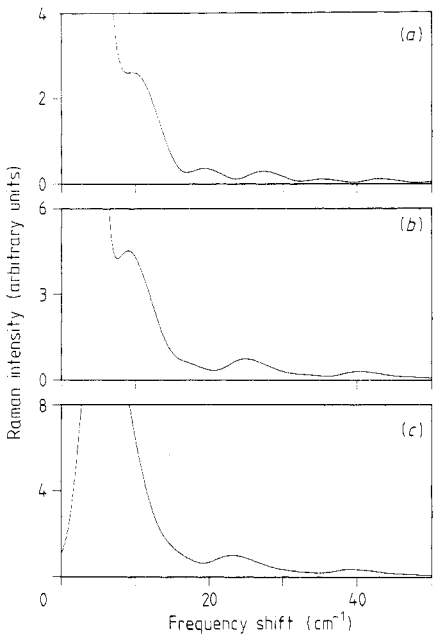

Figure 2. The calculated Raman spectrum for sample A (15 periods of Ge_2Si_2) on a 3000-atom Si substrate: (*a*) anchored outer surface ($\sigma = 1.0$), (*b*) weakly anchored outer surface ($\sigma = 0.1$), and (*c*) free outer surface ($\sigma = 0.0$).

experiment for the scattering events inside the crystal. The samples were placed in a helium atmosphere at room temperature and excited with 300 mW of 457.9 nm argon laser light polarised in the scattered light direction. The scattered light spectrum was recorded without polarisation analysis using a Spex 14018 double monochromator. The same spectrum was obtained when 30 mW of power was used for excitation.

Noting that the reduced Brillouin zone of Ge_2Si_2 superlattices would be comparable to those of pure Si or Ge, we do not expect to see the low-frequency folded acoustic modes found in conventional superlattices with periods of, for example, 50 or 100 Å (Lockwood *et al* 1987). In these ultra-thin superlattice materials the equivalent folded modes are in the frequency region of the Ge–Ge, Ge–Si and Si–Si bond optic vibrations. However, as shown in figure 1, an intense but broad peak is seen near 10 cm^{-1} together with a weaker broad peak near 20 cm^{-1}. There is an indication of another very weak peak near 40 cm^{-1}. The peak near 10 cm^{-1} is very strong, being almost a third of the height of the Brillouin peak, and contains a significant amount of spectral weight. All the peaks have a full width at half maximum (FWHM) of about 5 cm^{-1}. We interpret these new, broad, intense features as resonant phonon modes arising from the interaction between the continuum of acoustic modes of the Si substrate and the quasi-localised modes in the superlattice.

The theory of impurity modes in lattice dynamics is well understood via the Green function formulation of host–defect interactions (Maradudin 1965), especially in the case of a single substitutional impurity atom of mass m_1 connected to nearest neighbours with force constants f_1. If the original lattice consisted of atoms of mass m and nearest-

neighbour force constants f, the nature of the new modes is governed by the mass defect parameter $e = 1 - m_I/m$, and the force constant defect parameter $\gamma = 1 - f_I/f$. Stiff substituents of light mass give rise to high-frequency localised modes outside the spectrum of the host lattice. Heavy substituents with smaller f_I give rise to band modes within the continuum of the host lattice and usually acquire a resonant character. The 'resonant mode' consists of an envelope of modes, in each of which the defect vibrates with significantly enhanced amplitude. The 'width' of the resonant mode is proportional to $(1-\gamma)^{1/2}(1-e)^{1/2}\Omega$, where Ω is the frequency of the resonance (Genzel *et al* 1965).

In the present problem, the 'defect' is the thin superlattice layer of thickness l attached to the (001) surface of the essentially semi-infinite substrate layer. The close analogy to resonant states in electron tunnelling across heterostructures, and to the Fano (1961) and Anderson (1961) models for the interaction of localised modes with a continuum should be noted. The simplest model for the localised modes of the finite superlattice is to take them to be those of a string of length l with fixed boundaries. The modes have energies E_n, with $E_n = qV_{SL}$, and $q = n\pi/l$ for $n = 1, 2, 3, \ldots$, where V_{SL} is an average superlattice sound velocity. Using reasonable values for the sound velocities in Si and in the superlattice, and $l \simeq 90$ Å for the 15-period Ge_2Si_2 superlattice, peak frequencies and widths in qualitative agreement with the experiment are obtained. However, to obtain a more flexible approach where the effects of boundary conditions could be easily studied, we have adopted a simple linear chain model with nearest-neighbour interactions (Dean 1967, Barker and Sievers 1975). The linear chain model uses $N \simeq 3000$ atoms of Si to model the substrate. The substrate force constant f_{Si} was adjusted to give the experimental Brillouin frequency of 5.3 cm^{-1} yielding $f_{Si} = 1.62 \times 10^5$ dyn cm^{-1}, and the Si monolayer thickness was taken to be 1.36 Å. If the number of atoms N is significantly small, the calculated Brillouin peak acquires structure and a FWHM greater than the experimental width of 0.8 cm^{-1} limited by the resolution of the instrument. The Ge_mSi_n superlattice layer was modelled with the Si–Si, Si–Ge and Ge–Ge bond lengths taken to be 1.36, 1.41 and 1.46 Å respectively (Feldman *et al* 1987). The nearest-neighbour force constants $f_{Si}, f_{Ge}, f_{Si-Ge}$ were all taken to be f_{SL}, whose value was adjusted to obtain agreement with the experimental spectrum. The theoretical Raman spectrum was calculated from the mode frequencies ω_j and eigenvectors $u_j(z)$ obtained from the linear chain model and by invoking a photoelastic coupling mechanism (Colvard *et al* 1985). The intensity of the Raman scattered light is then given by

$$I(\omega) \propto \sum_j \frac{\Gamma/\pi}{(\omega-\omega_j)^2+\Gamma^2}\left[(n(\omega_j)+1)/\omega_j\right]\left|\int_{-\infty}^{+\infty} e^{-iqz}\,P(z)\,\frac{\partial u_j(z)}{\partial z}\right|^2 \tag{1}$$

where Γ is a broadening parameter, $n(\omega_j)$ is the Bose factor, q is the change in photon momentum in the Raman scattering and $P(z)$ is the photoelastic constant. We have used a constant value P_1 for the substrate and $P_2 = 10P_1$ for the superlattice layer. A single (average) value of $P(z)$ has been used for the whole superlattice, without distinguishing between Si_n and Ge_m, as the low-frequency spectrum is insensitive to such details. The photon scattering wavevector q for the 457.9 nm light was estimated to be 0.0125 $Å^{-1}$ using a refractive index of 4.595, appropriate to bulk silicon. It was found that the Raman spectrum calculated with 1000 atoms of substrate and $\Gamma = 0.5$ cm^{-1} is visually similar to that with 3000 atoms of substrate and $\Gamma = 0.2$ cm^{-1}. In figure 2 we show the spectrum calculated for a 15-layer superlattice of Si_2Ge_2 with the boundary condition on the outer Si layer varied via a parameter $\sigma = 0$ or 1 for a free or anchored surface, respectively.

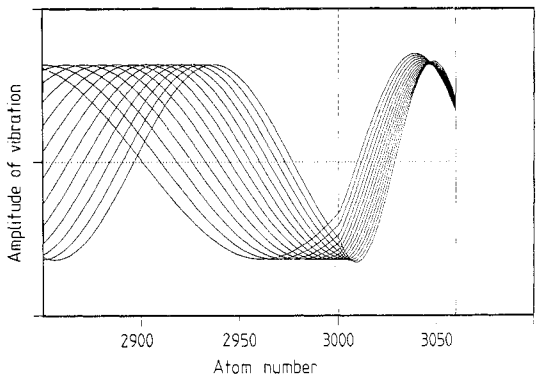

Figure 3. Some eigenvectors of modes contributing to the envelope of resonant phonons near 10 cm^{-1} in sample A, calculated from the linear chain model with a weakly anchored ($\sigma = 0.1$) surface, corresponding to figure 2(*b*). Atom 3000 is the substrate surface (broken vertical line) and atom 3060 is the superlattice surface (full vertical line).

That is, the equation of motion of the last atom ν corresponding to the surface monolayer is given by

$$m_{Si}\ddot{z}_\nu = f_{SL}(z_{\nu-1} - z_\nu) - f_{SL}\sigma z_\nu. \tag{2}$$

The first atom in the linear chain corresponding to the first monolayer of the Si substrate is anchored.

It can be seen from figure 2 that the form of the calculated spectrum is quite sensitive to the surface boundary conditions. Since the surface almost certainly contains an oxide layer, the assumption of a free surface ($\sigma = 0$) is a poor approximation. On the other hand, the oxide layer only loosely anchors the superlattice surface and hence an intermediate value of σ would be more appropriate. In the calculation, $\sigma = 0.1$ gives better detailed agreement with the experimental spectrum. The number of substrate atoms is not critical provided the rigid boundary condition on atom 1 is moved sufficiently far away from the interface. In figure 3 we show the variation in the amplitude of vibration as a function of atom number along the linear chain, for some of the modes which contribute to the resonant envelope near 10 cm^{-1}. These modes have just one node between the substrate–superlattice interface and the outer surface and hence correspond to the second localised mode (i.e., $q = n\pi/l$, $n = 2$, $l = 87.53$ Å) in the simple finite string model mentioned earlier. The $n = 1$ mode has shifted downwards in frequency and is concealed in the Brillouin line at 5.3 cm^{-1}. The apparent sensitivity of the appearance of the spectrum around 10 cm^{-1} to the value of σ arises from the fact that a free surface ($\sigma = 0$) shifts the resonant mode downwards and hence the 10 cm^{-1} peak merges into the Brillouin line rather than standing clear of it, as in the case when $\sigma = 1$.

The appearance of the low-frequency Raman spectrum is changed dramatically when the superlattice structure is capped with Si, as shown in figure 4(*a*) for the Ge_4Si_4 sample. A larger number of peaks of narrower width (approximately 3 cm^{-1}) is observed compared with the uncapped case. The calculated spectrum from the linear chain model reproduces this behaviour, and the best agreement with experiment was obtained for $\sigma = 0.1$ in both the capped and uncapped cases (see figure 4(*b*)). The appearance of a larger number of peaks in the same frequency range on capping with Si is simply the result of the increased length l of the combined system of superlattice plus cap and it

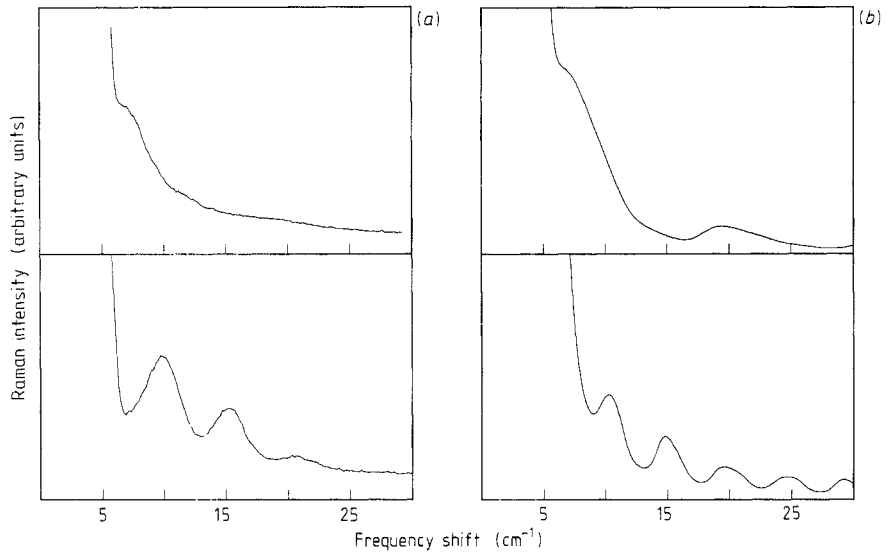

Figure 4. The (*a*) experimental, and (*b*) calculated ($\sigma = 0.1$) Raman spectrum of the 8-period Ge_4Si_4 superlattice. Upper curves, uncapped; lower curves, with a Si capping layer.

clearly demonstrates the resonant behaviour of the acoustic modes involved in Raman scattering.

In the case of the $Ge_{0.5}Si_{0.5}$ random alloy layer sample of 80 Å thickness deposited on the Si substrate, the resonant modes are again observable but the 10 cm^{-1} peak is less well separated from the steep Brillouin profile. In this case a linear chain model using the same force constants as for the superlattices and with a nearly free surface ($\sigma \simeq 0$) gives a spectrum in good accord with experiment. Some other value of the alloy layer force constant may possibly be in accord with a different value of σ, but such a study is meaningful only if a detailed attempt is made to model the oxide layer as well.

This study has revealed the importance of substrate–superlattice interactions as well as the effect of surface boundary conditions on the acoustic phonon Raman spectrum. The simple theory of the intensities of ordinary thick-layer superlattices (Colvard *et al* 1985) usually ignores such effects and is only qualitatively in accord with experiment. Attempts have been made to improve this by invoking interface broadening effects (Jusserand *et al* 1985), variation of individual layer thicknesses (Schwartz *et al* 1987) and other models (He *et al* 1988). We have examined theoretically the effect of the substrate and surface boundary condition on the phonon spectrum of ordinary superlattices and found that many weak spectral features, which do not appear in the simple theory but which appear in a finite superlattice calculation, can be enhanced in intensity when substrate and surface effects are included. A more detailed report of these studies will be published elsewhere.

We wish to thank H J Labbé for technical assistance in the Raman measurements.

References

Anderson P W 1961 *Phys. Rev.* **124** 41
Barker A S Jr and Sievers A J 1975 *Rev. Mod. Phys.* **47** Suppl. 2

Bevk J, Mannaerts J P, Feldman L C, Davidson B A and Ourmazd A 1986 *Appl. Phys. Lett.* **49** 286
Colvard C, Gant T A, Klein M V, Merlin R, Fischer R, Morkoc H and Gossard A C 1985 *Phys. Rev.* B **31** 2080
Dean P 1967 *J. Inst. Math. Applic.* **3** 98
Fano U 1961 *Phys. Rev.* **124** 1866
Feldman L C, Bevk J, Davidson B A, Gossman H-J and Mannaerts J P 1987 *Phys. Rev. Lett.* **59** 664
Flynn C P 1986 *Phys. Rev. Lett.* **57** 599
Genzel L, Renk K F and Weber R 1965 *Phys. Status Solidi* **12** 639
He J, Djafari-Rouhani B and Sapriel J 1988 *Phys. Rev.* B **37** 4086
Houghton D C, Lockwood D J, Dharma-wardana M W C, Fenton E W, Baribeau J-M and Denhoff M W 1987 *J. Cryst. Growth* **81** 434
Jusserand B, Alexandre F, Paquet D and LeRoux G 1985 *Appl. Phys. Lett.* **47** 301
Lockwood D J, Dharma-wardana M W C, Baribeau J-M and Houghton D C 1987 *Phys. Rev.* B **35** 2243
Maradudin A A 1965 *Rep. Prog. Phys.* **28** 347
Schwartz G P, Gualtieri G J, Sunder W A and Farrow L A 1987 *Superlatt. Microstruct.* **3** 523